

# Boosting RL-Based Visual Reasoning with Selective Adversarial Entropy Intervention

Yang Yu<sup>1</sup> Zhuangzhuang Chen<sup>1</sup> Siqi Wang<sup>1</sup> Lanqing Li<sup>2,3</sup> Xiaomeng Li<sup>1\*</sup>

<sup>1</sup> The Hong Kong University of Science and Technology

<sup>2</sup> Zhejiang Lab <sup>3</sup> The Chinese University of Hong Kong

eeyangyu@ust.hk, eexmli@ust.hk

## Abstract

Recently, reinforcement learning (RL) has become a common choice in enhancing the reasoning capabilities of vision-language models (VLMs). Considering existing RL-based finetuning methods, entropy intervention turns out to be an effective way to benefit exploratory ability, thereby improving policy performance. Notably, most existing studies intervene in entropy by simply controlling the update of specific tokens during policy optimization of RL. They ignore the entropy intervention during the RL sampling that can boost the performance of GRPO by improving the diversity of responses. In this paper, we propose Selective-adversarial Entropy Intervention, namely SaEI, which enhances policy entropy by distorting the visual input with the token-selective adversarial objective coming from the entropy of sampled responses. Specifically, we first propose entropy-guided adversarial sampling (EgAS) that formulates the entropy of sampled responses as an adversarial objective. Then, the corresponding adversarial gradient can be used to attack the visual input for producing adversarial samples, allowing the policy model to explore a larger answer space during RL sampling. Then, we propose token-selective entropy computation (TsEC) to maximize the effectiveness of adversarial attack in EgAS without distorting factual knowledge within VLMs. Extensive experiments on both in-domain and out-of-domain datasets show that our proposed method can greatly improve policy exploration via entropy intervention, to boost reasoning capabilities. Code will be released once the paper is accepted.

## 1. Introduction

Reinforcement learning (RL) advances large language models (LLMs) by enhancing their reasoning capabilities to realize planning, reflecting, and generalizing beyond mere memorization [13, 16, 30]. Motivated by this fact, RL-

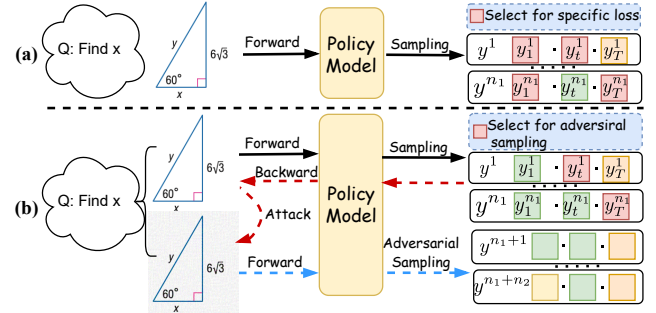


Figure 1. (a). Existing methods intervene in policy entropy from the perspective of policy optimization in RL, by controlling the update of specific tokens. (b). Our method utilizes entropy-guided adversarial samples to intervene in policy entropy from the perspective of RL sampling. Here,  $y^i$  represents a response, while  $y_t^i$  stands for a token in  $y^i$ .

based post-training has been explored to boost vision language models (VLMs), which equip LLMs with vision encoders, to solve complex problems like mathematical problems and code generation [9, 10].

Among advanced RL algorithms, group relative policy optimization (GRPO) [13] has attracted extensive attention, owing to its simplicity and scalability with competitive results. It allows LLMs to learn from a group of their own outputs by estimating advantages in a group-based manner. Notably, the diversity of their outputs is determined by policy exploration capacity, which is quantified by policy entropy in the RL sampling. Meanwhile, recent studies [7, 44] argue that GRPO cannot maintain a sufficient level of policy entropy during finetuning LLMs, which results in a performance plateau. To address this problem, entropy intervention has been proposed to improve exploratory ability. As shown in Fig. 1 (a), most existing works achieve entropy intervention by controlling the update of specific tokens during the policy optimization of RL. For example, Cui et al. [7] intervene in policy entropy by restricting the update of tokens with high covariances between the action probability

\*Corresponding author.

and the corresponding advantage value. Although entropy intervention during policy optimization has been well explored, existing works overlook entropy intervention during the RL sampling that can boost the performance of GRPO by improving the diversity of responses.

Intuitively, entropy intervention during RL sampling can be achieved by randomly disrupting the image-question pair. However, we found that the performance of random noise is sensitive to noise steps, as shown in Fig. 4. This further indicates that it will be hard to find suitable noise steps to achieve a precise control of entropy intervention. The reason lies in the fact that random disruption lacks an explicit relation to entropy. This leads to another natural question: *how to build relation between disruption and entropy?* To answer this question, we are motivated by the fact that adversarial attack provides an approach to link adversarial objective and adversarial sample through gradient back propagation. Considering this, we argue that entropy-guided adversarial samples can effectively control the degree of entropy, thus benefiting policy exploration.

Based on the above insights, we propose a novel Selective-adversarial Entropy Intervention (**SaEI**) that contains entropy-guided adversarial sampling (**EgAS**) and token-selective entropy computation (**TsEC**). Our key novelty lies in that we achieve controllable entropy intervention during RL sampling via an entropy-guided adversarial attack. Specifically, **EgAS** aims to enhance policy entropy by distorting the visual input with the adversarial objective coming from the entropy of sampled responses. As the adversarial gradient comes from policy entropy, adversarial samples can enforce the policy model to explore a larger response space during RL sampling. **TsEC** is further proposed to maximize the effectiveness of adversarial attack in **EgAS** without distorting factual knowledge within VLMs. **TsEC** constructs an entropy rank for all tokens and discards tokens with the highest and lowest rank. This approach considers the fact that tokens with the highest entropy are able to explore, while tokens with the lowest entropy contain factual knowledge [36], which should not be disrupted.

To the best of our knowledge, we are the first to explore adversarial samples for intervening in the policy entropy to benefit policy exploration of VLMs during RL-sampling. Our main contributions can be summarized as follows:

- We propose entropy-guided adversarial sampling (**EgAS**) that formulates the policy entropy as adversarial objective and attacks the visual input, allowing the policy model to explore a larger response space during RL sampling.
- We propose token-selective entropy computation (**TsEC**) to select valuable tokens via entropy rank for better constructing adversarial samples.
- Extensive experiments on popular in-domain (e.g., Geometry3K and MM-Eureka) and out-of-domain datasets (e.g., HallBench and MathVista) verify that our SaEI can

greatly boost reasoning capabilities in our entropy-guided adversarial manner during RL sampling.

## 2. Related Works

### 2.1. Reasoning in Language Models

Large Language Models (LLMs) [1, 8, 32] have achieved great success in processing language information, and become an important tool in our daily life. Furthermore, VLMs [3, 5, 17, 35] integrate the vision encoder into LLMs so that they can handle vision modality such as images and videos. Reasoning techniques [31, 37], also known as Chain-of-Thought (CoT) techniques, allow the model to think step-by-step before delivering the final prediction. Some studies [4, 41] suggest that reasoning techniques can greatly improve the performance of both LLMs and VLMs in solving complex problems. Therefore, reasoning tasks have attracted intensive research in this area.

Researchers have explored several approaches to stimulate the reasoning capacity of LLMs and VLMs. A stream of researches [27, 39] performs SFT on pre-collected long CoT data which follows specific steps, leading to improvement of reasoning capacity. The CoT data can be collected by guiding LLMs to generate structured reasoning templates—such as first descriptions and then conclusions [33, 41]. Other works generate the CoT data using advanced search methods such as Beam Search [38, 43], and Monte Carlo Tree Search (MCTS) [40, 42]. However, SFT-based reasoning approach suffers from two main challenges. First, it is costly to collect massive high-quality CoT data. Second, SFT-based reasoning models merely memorize the structured reasoning format and knowledge within CoT, struggling to adapt to unseen tasks [6].

Recently, reinforcement learning (RL) has emerged as another effective approach to activate reasoning capacity [13, 16, 30]. During RL training, the model first generates several candidate answers, which will be scored by a reward model. The model is optimized to encourage answers with high score while penalize answers with low score. Some works [14, 45, 46] deploy value-model-based to estimate advantage with a well-trained value model which enables precise, and step-wise credit assignment. However, it is challenging to train a high-quality value model. In contrast, value-model-free methods [13, 21, 44] eliminate the need for value model computation by utilizing rule-based reward function. Despite their implementation simplicity and robustness, these methods suffer from limitations like entropy collapse [50]. In this work, we focus on mitigating entropy collapse of value-model-free methods.

### 2.2. Reinforcement Learning in VLMs

Deepseek-R1 [13] proposes a new value-model-free RL algorithm, Group Relative Reinforcement Learning (GRPO),

which achieves great success in improving the reasoning capacity with massive verifiable questions. Inspired by the success of Deepseek-R1, a lot of works [11, 15, 26] utilize GRPO to enhance the general reasoning capacity of VLMs. These works first build a large scale multimodal dataset which consists of verifiable visual questions. They then deploy LLMs like GPT-4o to generate high-quality CoTs for a part of these questions. The questions with CoTs can be used for SFT, enabling MLLMs to imitate reasoning behavior in CoTs. Finally, they study how to combine SFT and RL to improve the reasoning capacity of MLLMs.

Besides visual conversation tasks, some other works demonstrate that RL can enhance reasoning in visual perception tasks, like referring object segmentation [19], object counting [20], and open vocabulary detection [22]. Unlike visual conversation tasks with free text answer, these visual perception tasks requires the model to predict answer in specific format. Therefore, these works focus on designing task-specific reward function to encourage MLLMs to accurately perceive images. For example, Seg-Zero [19] utilizes Bbox IoU Reward to encourage the predicted bbox to match the ground-truth bbox.

Some RL mechanism researches have focused on several limitations of GRPO like entropy collapse [7], training instability [44], reward bias [21], insufficient policy exploration [18], etc. Entropy Mechanism [7] notices the entropy collapse of reinforcement learning for Reasoning Language Models. It further proposes to mitigate entropy collapse by restricting the update of tokens with high covariances between advantage and action probability. In our work, we propose to intervene policy entropy with adversarial learning, disturbing the input of VLMs under the guidance of policy entropy.

### 3. Preliminaries

Derived from Proximal Policy Optimization (PPO) [29], GRPO is a value-model-free RL algorithm widely used to improve the reasoning capacity of VLMs through finetuning. GRPO gets rid of the value model in PPO by utilizing rule based reward function, which mainly consists of two types of rewards, i.e., accuracy reward and format reward. The former one evaluates if the response is accurate while the latter one enforces the model to output structured responses. For a pretrained VLM  $\pi_{\theta_{ref}}$  to be finetuned, GRPO uses it to initialize a policy model  $\pi_{\theta}$  under optimization and an old model  $\pi_{\theta_{old}}$  for sampling responses. Given an image-question pair  $q = (I, Q)$  and corresponding label  $y$ , the old model  $\pi_{\theta_{old}}$  first generates a group of  $n$  responses  $\{y^i\}_{i=1}^n$ . The rule-based reward function then gives group rewards  $\{R^i\}_{i=1}^n$  by evaluating these responses. Next, all tokens in a response share the same advantage  $\tilde{A}_t^i$

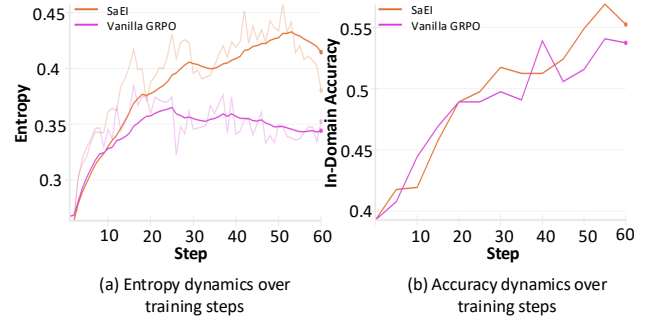


Figure 2. Comparison of our SaEI and vanilla GRPO in terms of entropy dynamics and accuracy dynamics over training steps. The comparison is conducted on the Geo3K dataset with group size  $n=12$ . The dark curves in (a) show data processed with an exponential moving average (EMA), while the light lines show the original data.

which is estimated by normalizing the group rewards:

$$\tilde{A}_t^i = \frac{R^i - \text{mean}(\{R^i\}_{i=1}^n)}{\text{std}(\{R^i\}_{i=1}^n)}. \quad (1)$$

The policy model  $\pi_{\theta}$  is optimized by maximizing the PPO-style objective:

$$\begin{aligned} \mathcal{J}_G(\theta) = & \mathbb{E}_{[q \sim P_D, \{y^i\}_{i=1}^n \sim \pi_{\theta_{old}}(\cdot|q)]} \\ & \frac{1}{n} \sum_{i=1}^n \frac{1}{|y^i|} \sum_{t=1}^{|y^i|} \left\{ \min \left[ \frac{\pi_{\theta}(y_t^i|q, y_{<t}^i)}{\pi_{\theta_{old}}(y_t^i|q, y_{<t}^i)} \tilde{A}_t^i, \right. \right. \\ & \left. \left. \text{clip} \left( \frac{\pi_{\theta}(y_t^i|q, y_{<t}^i)}{\pi_{\theta_{old}}(y_t^i|q, y_{<t}^i)}, 1 - \epsilon, 1 + \epsilon \right) \tilde{A}_t^i \right] - \beta D_{kl} \right\}, \end{aligned} \quad (2)$$

where  $D_{kl}$  measures the KL divergence between the policy model  $\pi_{\theta}$  and the pretrained VLM  $\pi_{\theta_{ref}}$ .  $\epsilon$  controls the clipping range to stabilize the training.

## 4. Methods

### 4.1. Overview

Previous studies [7] reveal that GRPO can benefit from a sufficient level of policy entropy. However, as shown in Fig. 2, vanilla GRPO can not maintain a sufficient level of policy entropy during finetuning VLMs for mathematical problems. To improve policy entropy, this paper provides a new perspective from RL sampling to intervene in policy entropy, instead of previous studies that control the update of specific tokens during policy optimization of RL. Specifically, we introduce Selective-adversarial Entropy Intervention (SaEI) to sample responses with entropy-driven adversarial samples. As illustrated in Fig. 3, SaEI takes policy entropy as an adversarial objective and backpropagates the gradient of the adversarial objective to disturb the input.

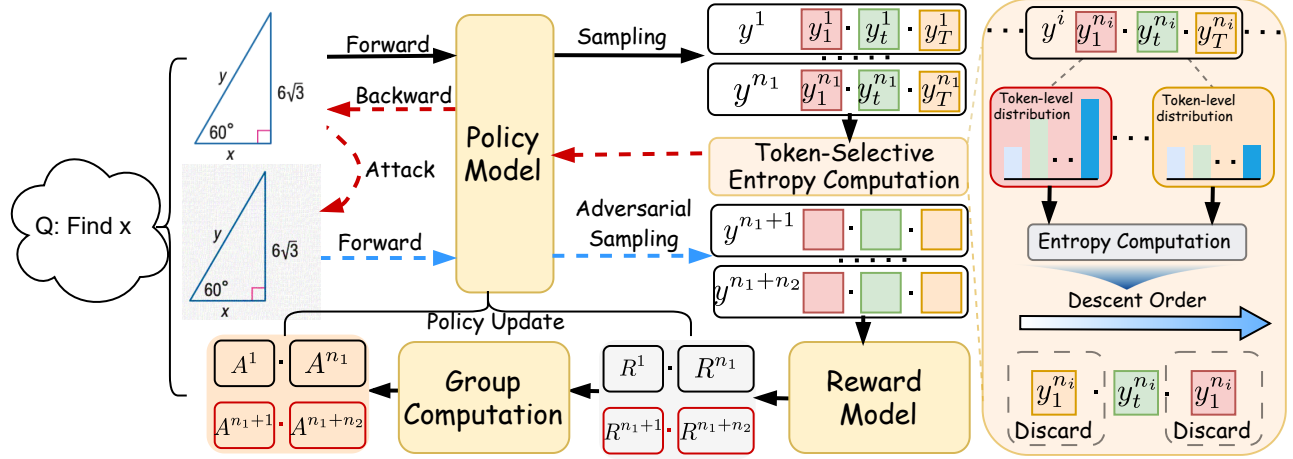


Figure 3. Overview of our proposed Selective adversarial Entropy Intervention (SaEI). It consists of entropy-guided adversarial sampling (EgAS) and token-selective entropy computation (TsEC). EgAS intervenes in policy entropy from the perspective of RL sampling, by taking entropy as an adversarial objective to disrupt visual input with the corresponding gradient. TsEC discards tokens with the highest and lowest entropy, while keeping tokens with moderate entropy for the entropy computation of the adversarial objective.

A selective adversarial is further proposed in SaEI to select tokens with an appropriate entropy pattern for the calculation of the adversarial objective. As shown in Fig.2, our SaEI can improve policy exploration by adequately increasing policy entropy during training. With better policy exploration, SaEI substantially outperforms vanilla GRPO.

#### 4.2. Entropy-guided Adversarial Sampling

To encourage policy exploration in RL sampling, SaEI introduces entropy-guided adversarial sampling, as shown in Fig.3. In RL sampling, the policy model  $\pi_{\theta_{old}}$  generates a group of  $n$  responses  $\{y^i\}_{i=1}^n$  for the image-question pair  $q = (I, Q)$ . We calculate the average of token-wise entropy values to quantify policy entropy:

$$\begin{aligned} \mathcal{H}(\pi_{\theta_{old}}, \{y^i\}_{i=1}^n) &= -\mathbb{E}_{\{y^i\}_{i=1}^n, \pi_{\theta_{old}}} [\log \pi_{\theta_{old}}(y_t^i | q, y_{<t}^i)] \\ &= -\frac{1}{n} \sum_{i=1}^n \frac{1}{|y^i|} \sum_{t=1}^{|y^i|} \mathbb{E}_{y_t^i \sim \pi_{\theta_{old}}} [\log \pi_{\theta_{old}}(y_t^i | q, y_{<t}^i)]. \end{aligned} \quad (3)$$

Intuitively, we can intervene in policy entropy by disrupting the image-question pair  $q$ . However, random disruption  $q$  lacks explicit relation between entropy intervention so that it cannot precisely control the direction and degree of entropy intervention. Adversarial learning provides an approach to link adversarial objective and adversarial disruption (or adversarial attack) through gradient back propagation. Based on adversarial learning, we take policy entropy in Eq.3 as adversarial objective and back propagate its gradient to  $q$  for disruption.  $q$  is composed of an image  $I$  and a textual question  $Q$ . The continuous nature and high dimensionality of the visual space make it widely acknowledged that visual adversarial examples are ubiquitous

and can be easily generated [28]. In contrast, adversarial disruption in textual domain is generally more demanding and might incurring consequences like generating abnormal texts [2, 48]. Therefore, we disrupt the visual input  $I$  in our adversarial sampling.

In our adversarial RL sampling, we first generate a group of  $n_1$  responses  $\{y^i\}_{i=1}^{n_1}$  based on clean image  $I$ . Then we calculate policy entropy  $\mathcal{H}(\pi_{\theta_{old}}, \{y^i\}_{i=1}^{n_1})$  of these responses with Eq.3. We take  $\mathcal{H}(\pi_{\theta_{old}}, \{y^i\}_{i=1}^{n_1})$  as adversarial objective to be enlarged and apply the projected gradient descent (PGD) attack [25] to obtain adversarial image in an iterative manner:

$$I_{adv}^{t+1} = I_{adv}^t + \alpha \cdot \text{sign}(\nabla_{I_{adv}^t} - \mathcal{H}(\pi_{\theta_{old}}, \{y^i\}_{i=1}^{n_1})), \quad (4)$$

where  $t$  indexes the iteration,  $\text{sign}(\cdot)$  is the sign function, and  $\alpha$  is a negative scalar representing the step size. By subtracting gradient from  $-\mathcal{H}(\pi_{\theta_{old}}, \{y^i\}_{i=1}^{n_1})$ , the obtained  $I_{adv}$  is able to encourage policy exploration with the increased policy entropy.

With the adversarial image  $I_{adv}$ , we generate another group of  $n_2$  responses  $\{y^i\}_{i=1}^{n_2}$  using adversarial image-text pair  $q_{adv} = (I_{adv}, Q)$ . Note that the question  $Q$  keeps unchanged. We then mix the two responses  $\{y^i\}_{i=1}^{n_1}$  and  $\{y^i\}_{i=1}^{n_2}$  together to form a new group of responses  $\{y^i\}_{i=1}^{n_1+n_2} = \{\{y^i\}_{i=1}^{n_1} \cup \{y^i\}_{i=1}^{n_2}\}$ . A group of rewards are calculated by the reward function  $\{R^i\}_{i=1}^{n_1+n_2} = \{\{R^i\}_{i=1}^{n_1} \cup \{R^i\}_{i=1}^{n_2}\}$ . The token advantages for  $\{y^i\}_{i=1}^{n_1+n_2}$  are estimated as:

$$\tilde{A}_t^i = \frac{R^i - \text{mean}(\{R^i\}_{i=1}^{n_1+n_2})}{\text{std}(\{R^i\}_{i=1}^{n_1+n_2})}. \quad (5)$$



Our policy optimization objective is defined:

$$\begin{aligned} \mathcal{J}(\theta) = & \mathbb{E}_{[q \sim P_D, \{\{y_i\}_{i=1}^{n_1} \sim \pi_{\theta_{\text{old}}}(\cdot|q) \cup \{y_i\}_{i=1}^{n_2} \sim \pi_{\theta_{\text{old}}}(\cdot|q_{adv})\}]} \\ & \frac{1}{n_1 + n_2} \sum_{i=1}^{n_1+n_2} \frac{1}{|y^i|} \sum_{t=1}^{|y^i|} \left\{ \min \left[ \frac{\pi_{\theta}(y_t^i|q, y_{<t}^i)}{\pi_{\theta_{\text{old}}}(y_t^i|q/q_{adv}, y_{<t}^i)} \tilde{A}_t^i, \right. \right. \\ & \left. \left. \text{clip} \left( \frac{\pi_{\theta}(y_t^i|q, y_{<t}^i)}{\pi_{\theta_{\text{old}}}(y_t^i|q/q_{adv}, y_{<t}^i)}, 1 - \epsilon, 1 + \epsilon \right) \tilde{A}_t^i \right] - \beta D_{kl} \right\}. \end{aligned} \quad (6)$$

Note that we use only clean images  $I$  for the calculation of current policy likelihood  $\pi_{\theta}(y_t^i|q, y_{<t}^i)$ , because current policy model  $\pi_{\theta}$  should be optimized using images following original distribution of  $I$ . Given the fact that we sample responses with both clean images  $I$  and adversarial images  $I_{adv}$ , herein, we use both  $I$  and  $I_{adv}$  for the calculation of  $\pi_{\theta_{\text{old}}}(y_t^i|q/q_{adv}, y_{<t}^i)$ , to make  $\pi_{\theta_{\text{old}}}(y_t^i|q/q_{adv}, y_{<t}^i)$  follow the distribution of our actual sampling policy. Our method only modifies the RL sampling, keeping the optimization objective in the RL policy update unchanged.

### 4.3. Token-Selective Entropy Computation

Our adversarial sampling is guided by policy entropy  $\mathcal{H}(\pi_{\theta_{\text{old}}}, \{y^i\}_{i=1}^n)$ , which is calculated from token-wise entropy values. As illustrated by Wang et al. [36], tokens with varying entropy patterns impact reasoning performance in different way, i.e., the tokens with the lowest entropy primarily complete the ongoing linguistic structures with factual knowledge memorized by LLMs, while the tokens with the highest entropy function as pivotal decision points that determine the direction of reasoning trajectories. The tokens with moderate tokens blend continuation and directing functions to varying degrees.

Inspired by Wang et al. [36], we assume that using adversarial samples to intervene in tokens with varying entropy patterns can impact our adversarial sampling in different ways. For the tokens with the lowest entropy, entropy intervention might distort factual knowledge by increasing their uncertainty. Since the tokens with the highest entropy are able to explore, it is dispensable to intervene in their entropy. Therefore, we equally divide tokens within a response into three groups based on their entropy values, resulting in groups of low, moderate, and high entropy. We introduce the token-selective entropy computation as shown in Fig.3, which only selects the tokens in the group of moderate entropy for the calculation of the adversarial objective, discarding the tokens in the groups of high and low entropy:

$$\begin{aligned} \mathcal{H}(\pi_{\theta_{\text{old}}}, \{y^i\}_{i=1}^{n_1}) = & -\frac{1}{n_1} \sum_{i=1}^{n_1} \frac{1}{|\hat{y}^i|} \sum_{t=1}^{|\hat{y}^i|} \mathbb{E}_{\hat{y}_t^i \sim \pi_{\theta_{\text{old}}}} [\log \pi_{\theta_{\text{old}}}(\hat{y}_t^i|q, y_{<t}^i)], \quad (7) \\ \text{s.t. } & \frac{1}{3} * |\hat{y}^i| < \text{rank}(\hat{y}_t^i) < \frac{2}{3} * |\hat{y}^i|. \end{aligned}$$

## 5. Experiments

In this section, we first introduce the datasets used for training, baseline methods, and benchmark used for evaluation. Then we present and analyze the comparison with baseline methods. Lastly, we conduct ablation studies to analyze our method in detail.

### 5.1. Datasets and Benchmarks

Our experiments are conducted with two mathematics related datasets: Geometry3K [23] and MM-Eureka [26]. Geometry3K is a dataset focusing on geometric problem, consisting of 2.1K training samples and 0.6K test samples. MM-Eureka is a multimodal mathematical K-12 level dataset, composed of 15.6K training samples and 2K test samples. All answers in these two datasets appear in free-text format to avoid model guessing.

Herein, we mainly evaluate model performance along two dimensions. More specifically, we consider the two test sets from Geometry3K and MM-Eureka as in-domain test sets. Additionally, given the renowned generalizability of reinforcement learning (RL), we evaluate our model on the following four out-of-domain visual reasoning benchmarks: MathVerse [47], MathVision [34], MathVista [24], and HallusionBench [12]. These benchmarks encompass a wide range of tasks involving mathematical reasoning and visual perception. We also report the average accuracy of these four benchmarks to get an overall evaluation. For questions with free-form ground truths, we employ the MathRuler to judge the prediction, while for questions with multiple-choice ground truths, we utilize the Gemini-2.0-Flash-001 to parse the prediction.

### 5.2. Baseline Methods

We compare our method with vanilla GRPO [13], KL-Cov proposed by Cui et al. [7], and NoisyRollout [18]. KL-Cov is designed to intervene in policy entropy by controlling the update of tokens with high covariances between the action probability and the corresponding advantage value during policy optimization of RL. NoisyRollout tries to improve GRPO by adding Gaussian noise to visual input and controlling noise strength with an annealing strategy. For both datasets, vanilla GRPO and KL-Cov use the group size of  $n = 12$ , while NoisyRollout and our SaEI use the group size of  $n_1 = 6, n_2 = 6$  for training. For a fair comparison, we reproduce vanilla GRPO, NoisyRollout, and KL-Cov following the default settings and general hyper-parameters of EasyR1, which is the same as our SaEI.

### 5.3. Implementation Details

We implement our method based on a widely used EasyR1 [49] codebase. We choose Qwen2.5-VL-7B-Instruct as our base model, because it demonstrates robust foundational abilities, making it an ideal candidate for RL finetuning.

Table 1. Comparison with existing methods on MM-Eureka. We report the mean and standard variation of 3 runs. All results are reported in percentages (%). † indicates that the model is not finetuned. Vanilla GRPO and KL-Cov use the group size of  $n = 12$ , while NoisyRollout and our SaEI use the group size of  $n_1 = n_2 = 6$ , resulting in a total group size of  $n = 12$  for fair comparison.

Method	MM-Eureka	HalluBench	MathVista	MathVerse	MathVision	OOD Avg.
Qwen2.5-VL-7B-Instruct †	41.70	64.00	67.14	42.87	25.95	49.99
Vanilla GRPO (Nature’25) [13]	$62.45 \pm 1.57$	$70.48 \pm 0.43$	$71.67 \pm 0.67$	$50.95 \pm 0.57$	$27.50 \pm 0.74$	55.15
NoisyRollout (NeurIPS’25) [18]	$62.93 \pm 0.08$	$71.33 \pm 0.61$	<b><math>74.16 \pm 0.67</math></b>	$47.74 \pm 0.94$	$27.96 \pm 0.12$	55.30
KL-Cov [7]	$63.34 \pm 4.51$	$70.67 \pm 1.07$	$71.60 \pm 1.25$	$50.97 \pm 0.36$	$28.60 \pm 0.82$	55.46
SaEI (Ours)	<b><math>64.45 \pm 1.26</math></b>	<b><math>71.85 \pm 0.46</math></b>	$72.10 \pm 0.40$	<b><math>51.06 \pm 0.28</math></b>	<b><math>29.21 \pm 0.32</math></b>	<b>56.05</b>

Table 2. Comparison with existing methods on Geometry3K. The group size is the same as Tab. 1. The best results are marked in bold.

Method	Geometry3K	HalluBench	MathVista	MathVerse	MathVision	OOD Avg.
Qwen2.5-VL-7B-Instruct†	39.27	64.00	67.14	42.87	25.95	49.99
Vanilla GRPO (Nature’25) [13]	$54.02 \pm 0.08$	$70.18 \pm 0.46$	$70.37 \pm 0.57$	$50.63 \pm 0.35$	$27.61 \pm 0.23$	54.70
NoisyRollout (NeurIPS’25) [18]	$54.74 \pm 1.26$	$70.11 \pm 0.45$	$70.67 \pm 0.45$	$46.24 \pm 0.78$	$27.70 \pm 0.35$	53.68
KL-Cov [7]	$55.91 \pm 0.17$	$68.31 \pm 3.07$	$71.33 \pm 0.67$	<b><math>51.40 \pm 0.89</math></b>	$27.92 \pm 0.33$	54.74
SaEI (Ours)	<b><math>56.18 \pm 0.51</math></b>	<b><math>70.38 \pm 0.36</math></b>	<b><math>71.53 \pm 0.72</math></b>	$51.15 \pm 0.25$	<b><math>28.17 \pm 0.47</math></b>	<b>55.31</b>

Table 3. Comparison with KL-Cov on Geometry3K with the group size of 8.

Method	Group Size	Geometry3K
Vanilla GRPO	$n = 8$	$52.47 \pm 0.97$
KL-Cov	$n = 8$	$53.86 \pm 0.53$
SaEI(Ours)	$n = 8(n_1 = n_2 = 4)$	<b><math>55.02 \pm 0.10</math></b>

We deploy the default settings and hyper-parameters from EasyR1 to focus on the development of our algorithm. Therefore, we keep vision encoder updated during training. We use a rollout temperature of 1.0, a rollout batch size of 512, a global batch size of 128, a kl loss weight  $\beta$  of  $1e-2$ , and a learning rate of  $1e-6$ . Our policy loss is computed in *token\_mean* average mode. For our adversarial learning, the iteration number of the PGD attack  $T$  is set to 1. The step size of adversarial attack  $\alpha$  is set to  $-\frac{2}{255}$  and  $-\frac{3}{255}$  for MM-Eureka and Geometry3K, respectively. We run 60 steps for Geometry3K and 90 steps for MM-Eureka. We run each experiment three times and report its average and standard deviation. For evaluation, we again follow the default setting of EasyR1 to set the temperature to 0.6 and report the average pass@1 accuracy. We evaluate the model every 5 steps using in-domain test set during training, reporting the highest result. We then evaluate the model with the highest in-domain result on out-of-domain benchmarks. Our experiments are conducted using 8 H100 GPUs with 80G memory. The prompts used are presented in appendix.

#### 5.4. Comparison with Other Methods

As shown in Tab. 1, after training on the MM-Eureka dataset, the model trained using our method attains an accuracy of 64.45% on the in-domain test set, demonstrating a 2.00% improvement over the model trained with vanilla GRPO. Our method outperforms NoisyRollout with a margin of 1.52%, which demonstrates our adversarial images are more effective than randomly augmented images for improving policy exploration. Although intervening in policy entropy from different perspectives, our method also outperforms KL-Cov with a gap of 1.11%. The superiority of our method is further emphasized by its performance on out-of-domain benchmarks. Our method achieves a 1.37% improvement over the model trained with vanilla GRPO, and outperforms KL-Cov with 1.18% on HallusionBench. Our method also achieves the best results in terms of “OOD Avg.”. Although NoisyRollout attains the best result on MathVista, it achieves the lowest result on MathVerse. It is noteworthy that KL-Cov shows extremely high standard variation of 4.51% on MM-Eureka, which illustrates its instability during training. Our method not only outperforms KL-Cov regarding accuracy, but also shows superiority over KL-Cov in terms of training stability.

As shown in Tab. 2, our method again significantly improves the in-domain accuracy of 2.16% and slightly surpass the second best KL-Cov of 0.27%. Although our method is slightly left behind by KL-Cov on MathVerse, it outperforms KL-Cov on HallusionBench, MathVista, and

Table 4. Component analysis of SaEI. “Im.” is short for improvement.

EgAS	TsEC	Geometry3K	Im. over GRPO
		$52.47 \pm 0.97$	0
✓		$53.86 \pm 0.53$	1.39
✓	✓	<b><math>55.02 \pm 0.10</math></b>	<b>2.55</b>

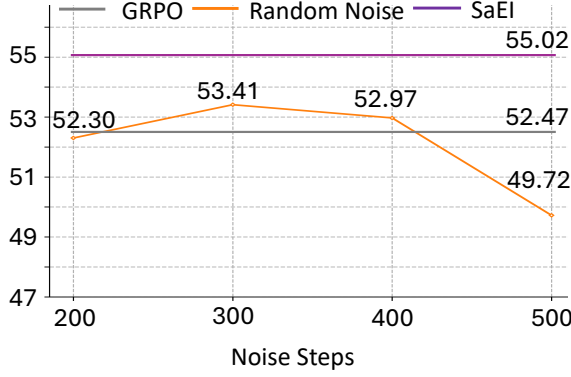


Figure 4. Comparison with random noise. We add multiple-step Gaussian noise to the image to create random noise.

MatchVision. Moreover, the improvement over KL-Cov is up to 2.05% on HallusionBench. As shown in Tab.3, we conduct comparison on Geometry3K with a smaller group size  $n = 8$ . The capacity of policy exploration declines with decreasing of the group size. Compared with KL-Cov, our method can better improve policy exploration under the smaller group size, with an improvement over vanilla GRPO of 2.55% vs. KL-Cov’s improvement over vanilla GRPO of 1.39%.

### 5.5. Ablation Studies

We conduct ablation studies on Geometry3K with the group size of  $n = 8$  and report in-domain accuracy.

**Component Analysis of SaEI.** Our SaEI consists of two main components, i.e., entropy-guided adversarial sampling (EgAS), and token-selective entropy computation (TsEC). For the experiment with only EgAS, we use all tokens of each sampled response to compute an adversarial objective whose gradient is then back-propagated to the visual input. Sampling with adversarial samples enables the policy model to explore a larger response space. As shown in Tab.4, after applying EgAS to vanilla GRPO, the performance is improved by 1.39% due to the improved policy exploration. Moreover, we use TsEC to discard the tokens with the lowest entropy to avoid distorting factual knowledge and those with the highest entropy, which are able to explore. The TsEC results in a more substantial improvement over vanilla GRPO, with gains of up to 2.55%.

**Comparison with Random Noise.** We compare our SaEI

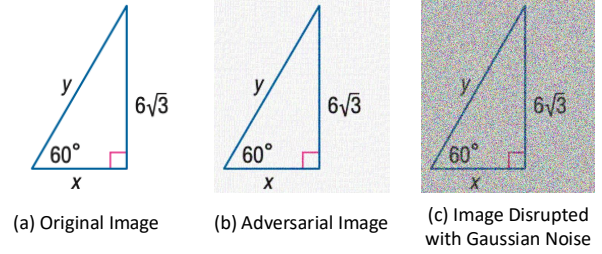


Figure 5. Visualization of an original image, its adversarial version (1 adversarial attack iteration with step size  $\alpha = 3/255$ ), and Gaussian noise (500-step) disrupted version.

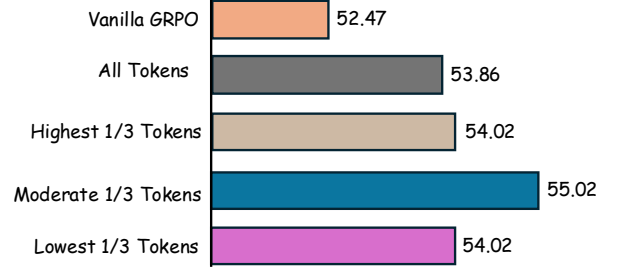


Figure 6. Ablation on token-selective entropy computation.

with random noise, which is created by adding multiple-step Gaussian noise to the image, as suggested by NoiseRollout [18]. For a fair comparison, we change the adversarial gradient SaEI adds to the image with random noise, while keep other experimental settings the same as SaEI. As shown in Fig.4, 300-step Gaussian noise leads to the best result (53.41%) among experiments with random noise. However, its result is 1.61% lower than SaEI, which demonstrates the superiority of SaEI. We can also observe that too weak random noise, i.e., 200-step Gaussian noise can hardly improve the result of GRPO due to its inability to intervene in policy entropy. However, too strong random noise, i.e., 500-step Gaussian noise leads to an accuracy drop up to 2.75%. The reason is that too strong random noise distorts the distribution of original images too much as shown in Fig.5 (c), thus impeding the learning from original images. In contrast, our SaEI can effectively intervene in policy entropy without distorting original image too much, as shown in Fig.5 (b). The inefficiency of random noise comes from lacking explicit relation with policy entropy. In contrast, our SaEI directly links policy entropy and the model input through adversarial attack.

**Ablation on TsEC.** In Fig.6, we study our token-selective entropy computation (TsEC) by comparing taking different groups of tokens to compute entropy as adversarial objective in EgAS. Our motivation is that the tokens with the lowest entropy contains factual knowledge which should not

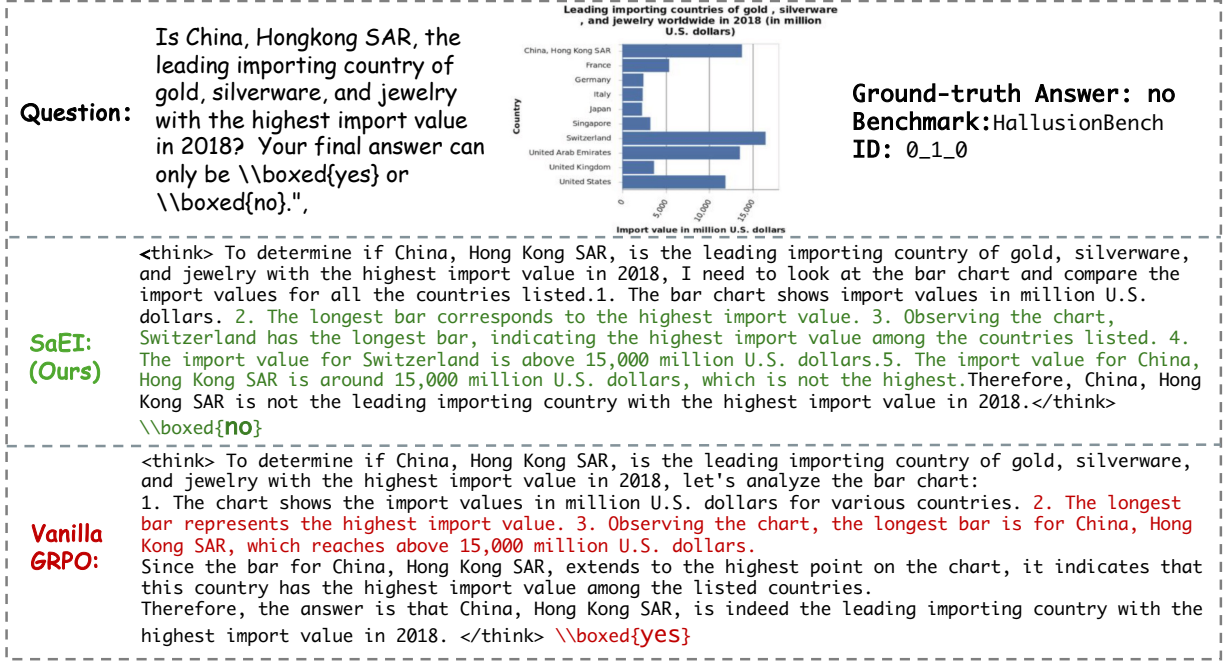


Figure 7. An example of a visual question-answer pair. The sample comes from HallusionBench, an OOD benchmark.

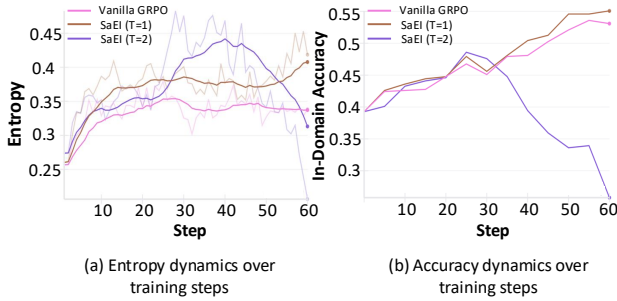


Figure 8. Ablation on iteration number of adversarial attack.

be distorted. The tokens highest entropy are able to explore and we do not need to enhance their entropy. Therefore, we equally divide the tokens within an response into three groups according to their entropy value, i.e. highest 1/3 tokens, moderate 1/3 tokens, and lowest 1/3 tokens. As shown in Fig. 6, taking “All tokens” leads to 1.39% improvement over vanilla GRPO and the improvement increases to 2.55% by taking “Moderate 1/3 tokens”. Taking “Highest 1/3 tokens” and “Highest 1/3 tokens” also lead to suboptimal results, compared with our method. The improvements of them are both 1.55%.

**Ablation on Adversarial Attack Iteration Number.** Our SaEI takes  $T = 1$  adversarial attack iteration, and we compare it with  $T = 2$ .  $T = 2$  causes a rapid entropy increase and a rapid accuracy decline after 30 steps. Since a larger  $T$  leads to training instability, we set  $T$  to 1, which is also

more computationally efficient.

## 5.6. Case Study

In Fig. 7, we present an example of visual question-answer pair. SaEI and vanilla GRPO are both trained on MM-Eureka dataset. Fig. 7 shows that even trained with a mathematics reasoning dataset, our SaEI model can provide correct reasoning processes and answers to general visual questions, even in cases where vanilla GRPO fails.

## 6. Conclusion

We investigate adversarial learning for entropy intervention in RL for enhancing the reasoning capabilities of VLMs. Then, we reveal that entropy-driven adversarial samples can effectively benefit policy exploration in RL. To this end, we propose Selective-adversarial Entropy Intervention (SaEI) to achieve entropy intervention in RL sampling, instead of previous studies that simply control the update of specific tokens during policy optimization of RL. SaEI contains the entropy-guided adversarial sampling (EgAS) that enables the policy model to explore a larger answer space by formulating the policy entropy as an adversarial objective and attacking the visual input. Then, token-selective entropy computation (TSEC) is proposed to maximize the effectiveness of adversarial attack in EgAS without distorting factual knowledge within VLMs. Extensive experiments show that our proposed EgAS can improve the generalization and robustness of current VLMs, leading to state-of-the-art performance across multiple visual reasoning benchmarks.



## References

- [1] Josh Achiam, Steven Adler, Sandhini Agarwal, Lama Ahmad, Ilge Akkaya, Florencia Leoni Aleman, Diogo Almeida, Janko Altenschmidt, Sam Altman, Shyamal Anadkat, et al. Gpt-4 technical report. *arXiv preprint arXiv:2303.08774*, 2023. 2
- [2] Moustafa Alzantot, Yash Sharma, Ahmed Elgohary, Bo-Jhang Ho, Mani Srivastava, and Kai-Wei Chang. Generating natural language adversarial examples. *arXiv preprint arXiv:1804.07998*, 2018. 4
- [3] Shuai Bai, Keqin Chen, Xuejing Liu, Jialin Wang, Wenbin Ge, Sibao Song, Kai Dang, Peng Wang, Shijie Wang, Jun Tang, et al. Qwen2. 5-vl technical report. *arXiv preprint arXiv:2502.13923*, 2025. 2
- [4] Maciej Besta, Nils Blach, Ales Kubicek, Robert Gerstenberger, Michal Podstawski, Lukas Gianinazzi, Joanna Gajda, Tomasz Lehmann, Hubert Niewiadomski, Piotr Nyczyk, et al. Graph of thoughts: Solving elaborate problems with large language models. In *Proceedings of the AAAI conference on artificial intelligence*, pages 17682–17690, 2024. 2
- [5] Zhe Chen, Weiyun Wang, Yue Cao, Yangzhou Liu, Zhangwei Gao, Erfei Cui, Jinguo Zhu, Shenglong Ye, Hao Tian, Zhaoyang Liu, et al. Expanding performance boundaries of open-source multimodal models with model, data, and test-time scaling. *arXiv preprint arXiv:2412.05271*, 2024. 2
- [6] Tianzhe Chu, Yuexiang Zhai, Jihan Yang, Shengbang Tong, Saining Xie, Dale Schuurmans, Quoc V Le, Sergey Levine, and Yi Ma. Sft memorizes, rl generalizes: A comparative study of foundation model post-training. *arXiv preprint arXiv:2501.17161*, 2025. 2
- [7] Ganqu Cui, Yuchen Zhang, Jiacheng Chen, Lifan Yuan, Zhi Wang, Yuxin Zuo, Haozhan Li, Yuchen Fan, Huayu Chen, Weize Chen, et al. The entropy mechanism of reinforcement learning for reasoning language models. *arXiv preprint arXiv:2505.22617*, 2025. 1, 3, 5, 6
- [8] Abhimanyu Dubey, Abhinav Jauhri, Abhinav Pandey, Abhishek Kadian, Ahmad Al-Dahle, Aiesha Letman, Akhil Mathur, Alan Schelten, Amy Yang, Angela Fan, et al. The llama 3 herd of models. *arXiv e-prints*, pages arXiv–2407, 2024. 2
- [9] Chanakya Ekbote, Vijay Lingam, Behrooz Omidvar-Tehrani, Luke Huan, Sujay Sanghavi, Anoop Deoras, and Stefano Soatto. Murphy: Reflective multi-turn reinforcement learning for self-correcting code generation in large language models. 2025. 1
- [10] Lishui Fan, Yu Zhang, Mouxian Chen, and Zhongxin Liu. Posterior-grpo: Rewarding reasoning processes in code generation. *arXiv preprint arXiv:2508.05170*, 2025. 1
- [11] Kaituo Feng, Kaixiong Gong, Bohao Li, Zonghao Guo, Yibing Wang, Tianshuo Peng, Junfei Wu, Xiaoying Zhang, Benyou Wang, and Xiangyu Yue. Video-rl: Reinforcing video reasoning in mllms. *arXiv preprint arXiv:2503.21776*, 2025. 3
- [12] Tianrui Guan, Fuxiao Liu, Xiyang Wu, Ruiqi Xian, Zongxia Li, Xiaoyu Liu, Xijun Wang, Lichang Chen, Furong Huang, Yaser Yacoob, et al. Hallusionbench: an advanced diagnostic suite for entangled language hallucination and visual illusion in large vision-language models. In *Proceedings of the IEEE/CVF Conference on Computer Vision and Pattern Recognition*, pages 14375–14385, 2024. 5
- [13] Daya Guo, Dejian Yang, Haowei Zhang, Junxiao Song, Peiyi Wang, Qihao Zhu, Runxin Xu, Ruoyu Zhang, Shirong Ma, Xiao Bi, et al. Deepseek-rl incentivizes reasoning in llms through reinforcement learning. *Nature*, 645(8081):633–638, 2025. 1, 2, 5, 6
- [14] Jingcheng Hu, Yinmin Zhang, Qi Han, Daxin Jiang, Xiangyu Zhang, and Heung-Yeung Shum. Open-reasoner-zero: An open source approach to scaling up reinforcement learning on the base model. *arXiv preprint arXiv:2503.24290*, 2025. 2
- [15] Wenxuan Huang, Bohan Jia, Zijie Zhai, Shaosheng Cao, Zheyu Ye, Fei Zhao, Zhe Xu, Yao Hu, and Shaohui Lin. Vision-rl: Incentivizing reasoning capability in multimodal large language models. *arXiv preprint arXiv:2503.06749*, 2025. 3
- [16] Aaron Jaech, Adam Kalai, Adam Lerer, Adam Richardson, Ahmed El-Kishky, Aiden Low, Alec Helyar, Aleksander Madry, Alex Beutel, Alex Carney, et al. Openai o1 system card. *arXiv preprint arXiv:2412.16720*, 2024. 1, 2
- [17] Haotian Liu, Chunyuan Li, Yuheng Li, and Yong Jae Lee. Improved baselines with visual instruction tuning. In *Proceedings of the IEEE/CVF conference on computer vision and pattern recognition*, pages 26296–26306, 2024. 2
- [18] Xiangyan Liu, Jinjie Ni, Zijian Wu, Chao Du, Longxu Dou, Haonan Wang, Tianyu Pang, and Michael Qizhe Shieh. Noisyrollout: Reinforcing visual reasoning with data augmentation. *arXiv preprint arXiv:2504.13055*, 2025. 3, 5, 6, 7
- [19] Yuqi Liu, Bohao Peng, Zhisheng Zhong, Zihao Yue, Fanbin Lu, Bei Yu, and Jiaya Jia. Seg-zero: Reasoning-chain guided segmentation via cognitive reinforcement. *arXiv preprint arXiv:2503.06520*, 2025. 3
- [20] Yuqi Liu, Tianyuan Qu, Zhisheng Zhong, Bohao Peng, Shu Liu, Bei Yu, and Jiaya Jia. Visionreasoner: Unified visual perception and reasoning via reinforcement learning. *arXiv preprint arXiv:2505.12081*, 2025. 3
- [21] Zichen Liu, Changyu Chen, Wenjun Li, Penghui Qi, Tianyu Pang, Chao Du, Wee Sun Lee, and Min Lin. Understanding rl-zero-like training: A critical perspective. *arXiv preprint arXiv:2503.20783*, 2025. 2, 3
- [22] Ziyu Liu, Zeyi Sun, Yuhang Zang, Xiaoyi Dong, Yuhang Cao, Haodong Duan, Dahua Lin, and Jiaqi Wang. Visual-rft: Visual reinforcement fine-tuning. *arXiv preprint arXiv:2503.01785*, 2025. 3
- [23] Pan Lu, Ran Gong, Shibiao Jiang, Liang Qiu, Siyuan Huang, Xiaodan Liang, and Song-Chun Zhu. Inter-gps: Interpretable geometry problem solving with formal language and symbolic reasoning. *arXiv preprint arXiv:2105.04165*, 2021. 5
- [24] Pan Lu, Hritik Bansal, Tony Xia, Jiacheng Liu, Chunyuan Li, Hannaneh Hajishirzi, Hao Cheng, Kai-Wei Chang, Michel Galley, and Jianfeng Gao. Mathvista: Evaluating mathematical reasoning of foundation models in visual contexts. *arXiv preprint arXiv:2310.02255*, 2023. 5

- [25] Aleksander Madry, Aleksandar Makelov, Ludwig Schmidt, Dimitris Tsipras, and Adrian Vladu. Towards deep learning models resistant to adversarial attacks. *arXiv preprint arXiv:1706.06083*, 2017. 4
- [26] Fanqing Meng, Lingxiao Du, Zongkai Liu, Zhixiang Zhou, Quanfeng Lu, Daocheng Fu, Botian Shi, Wenhai Wang, Junjun He, Kaipeng Zhang, et al. Mm-eureka: Exploring visual aha moment with rule-based large-scale reinforcement learning. *CoRR*, 2025. 3, 5
- [27] Niklas Muennighoff, Zitong Yang, Weijia Shi, Xiang Lisa Li, Li Fei-Fei, Hannaneh Hajishirzi, Luke Zettlemoyer, Percy Liang, Emmanuel Candès, and Tatsunori B Hashimoto. s1: Simple test-time scaling. In *Proceedings of the 2025 Conference on Empirical Methods in Natural Language Processing*, pages 20286–20332, 2025. 2
- [28] Xiangyu Qi, Kaixuan Huang, Ashwinee Panda, Peter Henderson, Mengdi Wang, and Prateek Mittal. Visual adversarial examples jailbreak aligned large language models. In *Proceedings of the AAAI conference on artificial intelligence*, pages 21527–21536, 2024. 4
- [29] John Schulman, Filip Wolski, Prafulla Dhariwal, Alec Radford, and Oleg Klimov. Proximal policy optimization algorithms. *arXiv preprint arXiv:1707.06347*, 2017. 3
- [30] ByteDance Seed, Jiaze Chen, Tiantian Fan, Xin Liu, Lingjun Liu, Zhiqi Lin, Mingxuan Wang, Chengyi Wang, Xiangpeng Wei, Wenyuan Xu, et al. Seed1. 5-thinking: Advancing superb reasoning models with reinforcement learning. *arXiv preprint arXiv:2504.13914*, 2025. 1, 2
- [31] Kimi Team, Angang Du, Bofei Gao, Bowei Xing, Changjiu Jiang, Cheng Chen, Cheng Li, Chenjun Xiao, Chenzhuang Du, Chonghua Liao, et al. Kimi k1. 5: Scaling reinforcement learning with llms. *arXiv preprint arXiv:2501.12599*, 2025. 2
- [32] Qwen Team et al. Qwen2 technical report. *arXiv preprint arXiv:2407.10671*, 2(3), 2024. 2
- [33] Omkar Thawakar, Dinura Dissanayake, Ketan Pravin More, Ritesh Thawkar, Ahmed Heakl, Noor Ahsan, Yuhao Li, Ilmuzz Zaman Mohammed Zumri, Jean Lahoud, Rao Muhammad Anwer, et al. Llamav-o1: Rethinking step-by-step visual reasoning in llms. In *Findings of the Association for Computational Linguistics: ACL 2025*, pages 24290–24315, 2025. 2
- [34] Ke Wang, Junting Pan, Weikang Shi, Zimu Lu, Houxing Ren, Aojun Zhou, Mingjie Zhan, and Hongsheng Li. Measuring multimodal mathematical reasoning with math-vision dataset. *Advances in Neural Information Processing Systems*, 37:95095–95169, 2024. 5
- [35] Peng Wang, Shuai Bai, Sinan Tan, Shijie Wang, Zhihao Fan, Jinze Bai, Keqin Chen, Xuejing Liu, Jialin Wang, Wenbin Ge, et al. Qwen2-vl: Enhancing vision-language model’s perception of the world at any resolution. *arXiv preprint arXiv:2409.12191*, 2024. 2
- [36] Shenzhi Wang, Le Yu, Chang Gao, Chujie Zheng, Shixuan Liu, Rui Lu, Kai Dang, Xionghui Chen, Jianxin Yang, Zhenru Zhang, et al. Beyond the 80/20 rule: High-entropy minority tokens drive effective reinforcement learning for llm reasoning. *arXiv preprint arXiv:2506.01939*, 2025. 2, 5
- [37] Xuezhi Wang and Denny Zhou. Chain-of-thought reasoning without prompting. *Advances in Neural Information Processing Systems*, 37:66383–66409, 2024. 2
- [38] Penghao Wu and Saining Xie. V?: Guided visual search as a core mechanism in multimodal llms. In *Proceedings of the IEEE/CVF Conference on Computer Vision and Pattern Recognition*, pages 13084–13094, 2024. 2
- [39] Qiong Wu, Xiangcong Yang, Yiyi Zhou, Chenxin Fang, Baiyang Song, Xiaoshuai Sun, and Rongrong Ji. Grounded chain-of-thought for multimodal large language models. *arXiv preprint arXiv:2503.12799*, 2025. 2
- [40] Yuxi Xie, Anirudh Goyal, Wenyue Zheng, Min-Yen Kan, Timothy P Lillicrap, Kenji Kawaguchi, and Michael Shieh. Monte carlo tree search boosts reasoning via iterative preference learning. *arXiv preprint arXiv:2405.00451*, 2024. 2
- [41] Guowei Wu, Peng Jin, Ziang Wu, Hao Li, Yibing Song, Lichao Sun, and Li Yuan. Llava-cot: Let vision language models reason step-by-step. In *Proceedings of the IEEE/CVF International Conference on Computer Vision*, pages 2087–2098, 2025. 2
- [42] Huanjin Yao, Jiaxing Huang, Wenhao Wu, Jingyi Zhang, Yibo Wang, Shunyu Liu, Yingjie Wang, Yuxin Song, Haocheng Feng, Li Shen, et al. Mulberry: Empowering mllm with o1-like reasoning and reflection via collective monte carlo tree search. *arXiv preprint arXiv:2412.18319*, 2024. 2
- [43] Shunyu Yao, Dian Yu, Jeffrey Zhao, Izhak Shafran, Tom Griffiths, Yuan Cao, and Karthik Narasimhan. Tree of thoughts: Deliberate problem solving with large language models. *Advances in neural information processing systems*, 36:11809–11822, 2023. 2
- [44] Qiying Yu, Zheng Zhang, Ruofei Zhu, Yufeng Yuan, Xiaochen Zuo, Yu Yue, Weinan Dai, Tiantian Fan, Gao-hong Liu, Lingjun Liu, et al. Dapo: An open-source llm reinforcement learning system at scale. *arXiv preprint arXiv:2503.14476*, 2025. 1, 2, 3
- [45] Yufeng Yuan, Yu Yue, Ruofei Zhu, Tiantian Fan, and Lin Yan. What’s behind ppo’s collapse in long-cot? value optimization holds the secret. *arXiv preprint arXiv:2503.01491*, 2025. 2
- [46] Yu Yue, Yufeng Yuan, Qiying Yu, Xiaochen Zuo, Ruofei Zhu, Wenyuan Xu, Jiaze Chen, Chengyi Wang, Tiantian Fan, Zhengyin Du, et al. Vapo: Efficient and reliable reinforcement learning for advanced reasoning tasks. *arXiv preprint arXiv:2504.05118*, 2025. 2
- [47] Renrui Zhang, Dongzhi Jiang, Yichi Zhang, Haokun Lin, Ziyu Guo, Pengshuo Qiu, Aojun Zhou, Pan Lu, Kai-Wei Chang, Yu Qiao, et al. Mathverse: Does your multi-modal llm truly see the diagrams in visual math problems? In *European Conference on Computer Vision*, pages 169–186. Springer, 2024. 5
- [48] Zhengli Zhao, Dheeru Dua, and Sameer Singh. Generating natural adversarial examples. *arXiv preprint arXiv:1710.11342*, 2017. 4
- [49] Yaowei Zheng, Junting Lu, Shenzhi Wang, Zhangchi Feng, Dongdong Kuang, and Yuwen Xiong. Easyrl: An efficient, scalable, multi-modality rl training framework, 2025. 5

- [50] Guanghao Zhou, Panjia Qiu, Cen Chen, Jie Wang, Zheming Yang, Jian Xu, and Minghui Qiu. Reinforced mllm: A survey on rl-based reasoning in multimodal large language models. *arXiv preprint arXiv:2504.21277*, 2025. [2](#)